JOURNÉE SCIENTIFIQUE D'URSI-FRANCE

Use of sparsity in nonlinear electromagnetic imaging: wavelet-based contrast source method

Y. Zhang[1], *M. Lambert*[1], *A. Fraysse*[2], *D. Lesselier*[2]

[1] *Université Paris-Saclay, CentraleSupélec, CNRS, Laboratoire de Génie Electrique et Electronique de Paris, 91192, Gif-sur-Yvette, France.*
Sorbonne Université, CNRS, Laboratoire de Génie Electrique et Electronique de Paris, 75252, Paris, France.
yarui.zhang@geeps.centralesupelec.fr, marc.lambert@geeps.centralesupelec.fr
[2] *Université Paris-Saclay, CNRS, CentraleSupélec, Laboratoire des signaux et systèmes, 91190, Gif-sur-Yvette, France.*
aurelia.fraysse@l2s.centralesupelec.fr, dominique.lesselier@l2s.centralesupelec.fr

key words: Inverse scattering, contrast source inversion (CSI), wavelet transform, sparsity regularization.

1 Introduction

Incorporation of the wavelet transform into classical inversion methods is attracting much attention due to its multiresolution capability and good compressive property. Several inversion methods such as the Born iterative method (BIM) [1], the contrast source inversion (CSI) method [2], and the subspace-based optimization method (SOM) [3] have already been investigated in the wavelet domain [6] [4] [5]. Our work aims at developing CSI method in the wavelet domain, at the same time, incorporating the sparsity into this framework due to the great potential of sparsity to effectively tackle the inverse problem and its robustness to noise.

2 Problem statement

The scenario considered is a time-harmonic two-dimensional (2D) electromagnetic scattering problem for transverse magnetic (TM) polarization. The object is located in the domain of interest D. N_s sources and N_r receivers are located on a line of observation S. The scattered electric field $E^{\text{diff}}(\mathbf{r}_r, \mathbf{r}_s)$ collected by a receiver placed at $\mathbf{r}_r$ and associated with the source placed at $\mathbf{r}_s$ satisfies the integral equation $E^{\text{diff}}(\mathbf{r}_r, \mathbf{r}_s) = \int_D G(\mathbf{r}_r, \mathbf{r}')J(\mathbf{r}', \mathbf{r_s})d\mathbf{r}'$, with $G(\mathbf{r}, \mathbf{r}')$ the Green's function and $J(\mathbf{r}, \mathbf{r_s}) = \chi(\mathbf{r})E(\mathbf{r}, \mathbf{r}_s)$ the equivalent current. The contrast function $\chi(\mathbf{r})$ is defined as $k^2(\mathbf{r}) - k_B^2$, where $k^2(\mathbf{r}) = \omega^2\epsilon_0\epsilon_r(\mathbf{r})\mu_0 + i\omega\mu_0\sigma(\mathbf{r})$, $k_B^2 = \omega^2\epsilon_0\mu_0$. ϵ_0 and μ_0 are the permittivity and permeability of air, respectively. $\epsilon_r(\mathbf{r})$ and $\sigma(\mathbf{r})$ are the relative permittivity and conductivity of the medium respectively, as $\mathbf{r} \in D$ is an observation point. ω is the angular frequency. $E^{\text{inc}}(\mathbf{r}, \mathbf{r}_s)$ is the incident electric field, and the total electric field $E(\mathbf{r}, \mathbf{r_s})$ can be obtained according to $E(\mathbf{r}, \mathbf{r_s}) = E^{\text{inc}}(\mathbf{r}, \mathbf{r}_s) + \int_D G(\mathbf{r}, \mathbf{r}')J(\mathbf{r}', \mathbf{r_s})d\mathbf{r}'$ $(\forall \mathbf{r} \in D)$.

Using the method of moments, the discretized version of the previous equations stands as $E_i^{\text{diff}}(\mathbf{r}) = G_S J_i(\mathbf{r})$ $\{i = 1, \ldots, N_s, \mathbf{r} \in S\}$ and $E_i(\mathbf{r}) = E_{\mathbf{r}}^{\text{inc}}(\mathbf{r}) + G_D J_i(\mathbf{r})$ $\{i = 1, \ldots, N_s, \mathbf{r} \in D\}$. G_S is the external mapping operator and G_D is the internal mapping operator. The inverse scattering problem is to retrieve $\chi(\mathbf{r})$ from $E^{\text{diff}}(\mathbf{r}_r, \mathbf{r}_s)$, which is nonlinear and ill-posed.

3 Wavelet-domain contrast source inversion method

Inspired from [4], we can apply the CSI method in the wavelet domain. First, let us define the wavelet transform as $\mathcal{W}$ and its inverse as $\mathcal{W}^*$. $\|\cdot\|_{Dw}^2$ and $\|\cdot\|_{Sw}^2$ indicate the norms on $L^2(S)$ and $L^2(D)$ in the wavelet domain. By combining previous equations, the data equation and the state equation are defined as $f_i = G_S(\mathcal{W}^*\gamma_i)$ and $\gamma_i = \mathcal{W}\{(\mathcal{W}^*\beta)E_i^{\text{inc}}\} + \mathcal{W}\{(\mathcal{W}^*\beta)G_D(\mathcal{W}^*\gamma_i)\}$, respectively, where $\gamma_i = \mathcal{W}J_i$, $\beta = \mathcal{W}\chi$. The cost function in the wavelet domain is given by

$$F(\gamma_1, \ldots \gamma_{N_s}, \beta) = \frac{\sum_{i=1}^{N_s} \|f_i - G_S(\mathcal{W}^*\gamma_i)\|_S^2}{\sum_{i=1}^{N_s} \|f_i\|_S^2} + \frac{\sum_{i=1}^{N_s} \|\mathcal{W}\{(\mathcal{W}^*\beta)E_i^{\text{inc}}\} + \mathcal{W}\{(\mathcal{W}^*\beta)G_D(\mathcal{W}^*\gamma_i)\} - \gamma_i\|_{Dw}^2}{\sum_{i=1}^{N_s} \|\mathcal{W}\{(\mathcal{W}^*\beta)E_i^{\text{inc}}\}\|_{Dw}^2} \quad (1)$$

The cost function consists of the normalized error of the data equation and state equation. It is minimized by alternatively updating χ and J_i in the wavelet domain (β, γ_i) using the conjugate-gradient (CG) method. The wavelet transform produces two sets of coefficients: approximation coefficients and detail coefficients. The first step of our approach is to

update only approximation coefficients to obtain a preliminary result. Then, we can determine the positions of significant wavelet coefficients based on this result, by employing the parent-child relationship [7] between approximation and detail wavelet coefficients with the threshold value T_1. The second step is to launch again the algorithm to update the significant detail coefficients and to get a finer result with the previous result being the initial model. At the same time, the soft-thresholding is applied with the threshold value T_2.

4 Numerical results

In the numerical simulations, the "Austria" profile which contains two disks and one ring is used. The true value of the relative permittivity of the object is 2 and it is 1 for the embedding medium. The region of interest D is $l = 1.33\lambda$ sided and the S is of radius $r = 2.5\lambda$, where λ is the wavelength in air. The frequency is $500\,\mathrm{MHz}$. Gaussian noise with SNR of $20\,\mathrm{dB}$ is added to the data. A positivity constraint is applied. The wavelet basis used in the simulations is the Haar wavelet, and the level of wavelet decomposition $J = 1$. The threshold value T_1 is the $85th$ percentile of approximation coefficients, and T_2 is set to the minimum value of the significant approximation coefficients. In the following, three

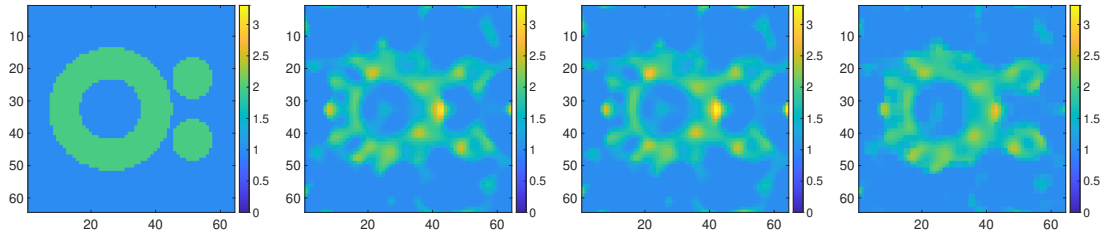

(a) Ground truth **(b)** CSI **(c)** W-CSI **(d)** W-CSI-ST

Figure 1: Real (left) and imaginary (right) parts of true model (a), and reconstructed model using CSI (b) and wavelet-domain CSI without (c) and with sparsity constraint (d) for $N_s = 6$ and $N_r = 18$.

methods are discussed including spatial-domain CSI, wavelet-domain CSI using all coefficients and wavelet-domain CSI using only significant wavelet coefficients with the soft-thresholding step respectively named as CSI, W-CSI and W-CSI-ST. As an illustration, a comparison of the final results for $N_s = 6$ and $N_r = 18$ is shown in Fig. 1. As expected, W-CSI-ST (Fig. 1d) provides a better and smoother result than CSI (Fig. 1b) and W-CSI (Fig. 1c) when using a small number of sources and receivers at a CPU time cost of $150\,\mathrm{s}$ for $K = 500$ compared to $22\,\mathrm{s}$ and $75\,\mathrm{s}$ respectively. By evaluating the relative error $err = \frac{\|\boldsymbol{\chi}_{\text{reconstructed}} - \boldsymbol{\chi}_{\text{true}}\|^2}{\|\boldsymbol{\chi}_{\text{true}}\|^2}$, the proposed method is proven to ensure better quality of reconstruction when N_s and N_r are small but about the same quality (at the price of increasing CPU time) when N_s and N_r increase. The machine that has been used has a processor such as: Intel Core i9 CPU@2.9 GHz.

5 Conclusion and future work

A new approach has been proposed in order to solve the inverse scattering problem with strong non-linearity by enforcing sparsity through the soft thresholding in the wavelet domain, which improves the quality of reconstruction. Future research will be on the accurate determination of hyperparameters as well as extension to far more complicated object profiles.

References

[1] Y. M. Wang and W. C. Chew, "An Iterative Solution of the Two-dimensional Electromagnetic Inverse Scattering Problem," *Int. J. Imag. Syst. Tech.* **1**, pp. 100–108, 1989, doi: 10.1002/ima.1850010111.

[2] P. M. van den Berg and A. Abubakar, "Contrast Source Inversion Method: State of Art," *Prog. Electromagn. Res.*, **34**, pp. 189-218, 2001. doi: 10.2528/PIER01061103.

[3] X. Chen, "Subspace-Based Optimization Method for Solving Inverse-Scattering Problems," *IEEE Trans. Geosci. Remote Sens.*, **48**, 1, pp. 42-49, 2010, doi: 10.1109/TGRS.2009.2025122.

[4] M. Li, O. Semerci, and A. Abubakar, "A Contrast Source Inversion Method in the Wavelet Domain," *Inverse Probl.*. **29**, 025015, 2013, doi: 10.1088/0266-5611/29/2/025015.

[5] T. Yin, Z. Wei, and X. Chen, "Wavelet Transform Subspace-Based Optimization Method for Inverse Scattering," *IEEE J. Multiscale Multiphys. Comput. Tech.*, **3**, pp. 176-184, 2018, doi: 10.1109/JMMCT.2018.2878483.

[6] Y. Sanghvi, H. Bisht, U. Khankhoje, V. Gadre, and S. Kulkarni, "Iteratively Reweighted $\ell 1$–$\ell 2$ Norm Minimization using Wavelets in Inverse Scattering," *J. Opt. Soc. Am. A*, **37**, pp. 889-889, 2020, doi: 10.1364/JOSAA.396227.

[7] J. M. Shapiro, "Embedded Image Coding using Zerotrees of Wavelet Coefficients," *IEEE Trans. Signal Process.*, **41**, 12, pp. 3445-3462, 1993, doi: 10.1109/78.258085.